enough to maintain the "normal" carbonyl base angle.

The C_2–C_3 bond length in cyclobutanone (1.567 (5) Å) is longer than the average sp^3–sp^3 C–C bonds in the five-, six-, and seven-membered rings. This long bond length in cyclobutanone reflects the strain of the ring system and is released as the rings get larger and larger. The results for cyclopropanone are included in the table for completeness; however, the special bonding environment in cyclopropane makes comparison with the other cyclic systems impossible.

The dynamic model analysis of the electron diffraction data indicates that for cyclopentanone the barrier to the conversion between the two twist forms is about 2 kcal/mol which is in good agreement with the results reported by Ikeda and Lord.[8] We do not wish to place too much emphasis on the results obtained for the dynamic model. For molecules such as cyclopentanone, where the barrier to interconversion is high, the electron diffraction analysis is simply not sensitive enough to determine good values for such energy parameters. The far-infrared data and its analysis by Ikeda and Lord provide a much better physical picture of the molecular dynamics than provided in this paper by electron diffraction.

Acknowledgment. We acknowledge The National Science Foundation, Grant CHE8111739, for their support of this research.

Supplementary Material Available: Correlation matrix and long and short camera distance data for cyclopentanone (4 pages). Ordering information is given on any current masthead page.

Tunneling Reaction Path for the Interaction of Silicon Atom and Water

Akitomo Tachibana,*† Masahiko Koizumi,‡ Hiroyuki Teramae,§ and Tokio Yamabe†,‡

Contribution from the Department of Hydrocarbon Chemistry, Faculty of Engineering, Kyoto University, Kyoto 606, Japan. *Received June 27, 1986*

Abstract: Ab initio molecular orbital (MO) calculations are carried out for the reaction path of a silicon atom and a water molecule. An intrinsic reaction coordinate (IRC) analysis for the potential energy surface reveals the following reaction mechanism. First a triplet silicon atom forms a triplet silicon–water adduct. Then a hydrogen of water in the adduct migrates to silicon to form the triplet HSiOH through proton tunneling. This migrated species may be converted to the singlet state by intersystem crossing. This picture is in close agreement with matrix isolation experiments.

I. Introduction

Recently, interactions and reactions of silicon-containing compounds have received much attention from both experimental and theoretical viewpoints.[1] In particular, the characteristic reaction pathway of silanone $H_2Si{=}O$ is a typical case study in silicon chemistry as a counterpart of formaldehyde H_2CO in hydrocarbon chemistry.[2-6] A variety of rearrangement channels both in the ground and excited states is available. Recent experimental study has proven that *trans*-HSiOH is the most stable species of the $[H_2SiO]$ system.[2,3] This is in accordance with predictions from previous theoretical studies.[4-6]

The rearrangement channel from silicon atom and water molecule is also interesting, because it is a model surface water reaction which may occur in the preparation of semiconductor or amorphous silicon devices in the electronics industry. In this direction of research, Ismail et al. carried out the experiment of the addition reaction of a silicon atom with water in an argon matrix and traced the IR spectra.[2] The mixture containing silicon, of which the ratio to water ($H_2O + D_2O$) and argon was 9:1:3300, immediately gave silicon–water adducts $Si{:}OH_2$, Si:OHD, and $Si{:}OD_2$ at 15 K. The IR spectra measured 7 h later for this mixture indicated the formation of insertion products HSiOH and HSiOD but no formation of DSiOH and DSiOD. The D_2O only formed the adduct $Si{:}OD_2$ upon thermal interaction with silicon. Photolysis using light of a wavelength greater than 400 nm was necessary for the formation of DSiOD. The thermal reaction rate of Si atom insertion into the OH bond, which is also regarded as the migration of hydrogen from water to silicon, is not affected by temperature. This suggests that the rate-determining step contains a tunneling process. Consequently, the following mechanism has been suggested: the ground state of atomic silicon, the triplet $Si(^3P)$, forms the silicon–water triplet adduct ($^3A''$). It rearranges to HSiOH (triplet) through a hydrogen atom tunneling maintaining the spin multiplicity. This is finally converted to the ground singlet state HSiOH ($^1A'$). Irradiation of the matrix causes the dissociation of HSiOH, HSiOD, and DSiOD to form silicon monoxide and molecular hydrogen or two hydrogen atoms.

In this paper, we study the following reaction processes of the silicon–water system, possessing these characteristic isotope effects mentioned above, by use of an ab initio molecular orbital (MO) method. The terms in parentheses after species indicate electronic

$$Si(^3P) + H_2O \rightarrow Si{:}OH_2(^3A'')(SiW(^3A'')) \quad (1)$$

$$Si(^1D) + H_2O \rightarrow Si{:}OH_2(^1A'')(SiW(^1A'')) \quad (2)$$

$$Si(^1S) + H_2O \rightarrow Si{:}OH_2(^1A')(SiW(^1A')) \quad (3)$$

$$SiW(^3A'') \rightarrow TS(\text{triplet}) \rightarrow HSiOH(\text{triplet}) \quad (4)$$

$$SiW(^1A'') \rightarrow TS(\text{open singlet}) \rightarrow HSiOH(\text{open singlet}) \quad (5)$$

$$SiW(^1A') \rightarrow TS(\text{closed singlet}) \rightarrow HSiOH(^1A') \quad (6)$$

*Present address: Department of Chemistry, University of North Carolina, Chapel Hill, NC 27514.

†Also belong to Division of Molecular Engineering, Graduate School of Engineering, Kyoto University, Kyoto 606, Japan.

‡Also belong to Institute for Fundamental Chemistry, 15 Morimoto-cho, Shimogamo, Sakyo-ku, Kyoto 606, Japan.

§Present address: NTT Electrical Communications Laboratories, Nippon Telegraph and Telephone Corporation, 3-9-11, Midori-cho, Musashino, Tokyo 180, Japan.

(1) Raabe, G.; Michl, J. *Chem. Rev.* **1985**, *85*, 419.

(2) Ismail, Z. K.; Hauge, R. H.; Fredin, L.; Kauffman, J. W.; Margrave, J. L. *J. Chem. Phys.* **1982**, *77*, 1617.

(3) (a) Withnall, R.; Andrews, L. *J. Am. Chem. Soc.* **1985**, *107*, 2567. Withnall, R.; Andrews, L. *J. Phys. Chem.* **1985**, *89*, 3261. (b) Glinski, R. J.; Gole, J. L.; Dixon, D. A. *J. Am. Chem. Soc.* **1985**, *107*, 5891.

(4) Kudo, T.; Nagase, S. *J. Phys. Chem.* **1984**, *88*, 2833.

(5) Sakai, S.; Jordan, K. D. *Chem. Phys. Lett.* **1986**, *130*, 103.

(6) Tachibana, A.; Fueno, H.; Yamabe, T. *J. Am. Chem. Soc.* **1986**, *108*, 4346.

0002-7863/87/1509-1383$01.50/0

Table I. Total Energies (hartree) and Zero-Point Energies (kcal/mol)

	total electronic energy				zero-point energy					
	$^3A''$[f]	$^3A''$[g]	$^1A''$[g]	$^1A'$[h]	$^3A''$[l]	$^1A''$[l]	$^1A'$[j]	$^3A''$[k]	$^1A''$[k]	$^1A'$[l]
Si	−288.83179	−288.88765	−288.86970	−288.83845						
H_2O	(−76.00987)[a]			−76.23115			14.4			13.5
SiW	−364.85847	−365.13929	−365.12219	−365.09760	16.0	15.9	15.5	15.2	15.1	14.8
TS[b]	−364.79088	−365.08945	−365.08102	−365.07954	11.5	11.3	11.4	11.0	10.5	10.9
t-HSiOH[c]	−364.88359	−365.15953		−365.22233[d]	13.6		14.1[e]	12.8		13.4

[a] Closed-shell singlet energy by RHF/6-31G*. [b] Electronic state has no symmetry. [c] Electronic state has no symmetry, except for $^1A'$. [d] Geometries from ref 4. [e] Taken from ref 4. [f] Geometry optimized by UHF/6-31G*. Energy by UHF/6-31G*. [g] Geometry optimized by UMP2/6-31G*. Energy by UMP4(SDTQ)/6-31G**. [h] Geometry optimized by RMP2/6-31G*. Energy by RMP4(SDTQ)6-31G**. [i] UHF/6-31G*. [j] RHF/6-31G*. [k] UMP2/6-31G*. [l] RMP2/6-31G*.

states. Reactions 1 and 4 are triplet state processes, and reactions 2,5 and 3,6 proceed on open- and closed-singlet state surfaces. We will use the abbreviations SiW and TS to mean silicon–water adduct and transition state, respectively. The tunneling path[7,8] for the reaction 4 is studied in detail by using the concept of Fukui's Intrinsic Reaction Coordinate (IRC)[8] in order to analyze the isotope effect.

II. Methods of Calculation

The MO calculations are carried out mainly with the GAUSSIAN 82 program package.[9] Geometry optimization of equilibrium points is performed by using the energy gradient method[10] based upon the Hartree–Fock theory with 6-31G* basis set.[11] Tracing of the IRC is carried out with HONDOG program[12] on the triplet UHF/6-31G* potential energy surface. Energetics of the reaction path are further refined by geometry reoptimization of equilibrium points by using Møller–Plesset second-order perturbation theory[13] with the 6-31G* basis set.

To obtain more accurate potential energy values at the MP2/6-31G* geometries, we also make use of Møller–Plesset fourth-order perturbation theory considering the contribution of single, double, triple, and quadruple substitutions[14] with the 6-31G** basis set: denoted as MP4(SDTQ)/6-31G**//MP2/6-31G*.

Vibrational analysis is performed by using the analytical second derivatives[13] based on HF/6-31G*//HF/6-31G* and the numerical differentiation of analytical MP2/6-31G* first derivative. We estimate the zero-point energy (ZPE) and the imaginary vibrational mode at TS which corresponds to the initial direction of the reaction path at TS.[8]

III. Results and Discussion

A. Geometries of Equilibrium Points. Figure 1 shows the optimized geometry of the reactants, products, and TS's for the reactions 4, 5, and 6. Figure 2 shows the displacement vector and frequency of the imaginary vibrational mode on each TS.

The silicon–water adduct SiW has a flapped structure as shown in Figure 1 (parts a, b, and c). For the reactions 1, 2, and 3, we cannot find any TS's. The SiW($^1A'$) has a flatter structure than the SiW($^1A''$) which is almost the same structure as SiW($^3A''$). For the reactions 4, 5, and 6, the TS's are obtained as nonplanar structures as shown in Figure 1 (parts d, e, and f). The structures of three TS's with C_1 symmetry resemble each other. The TS(open

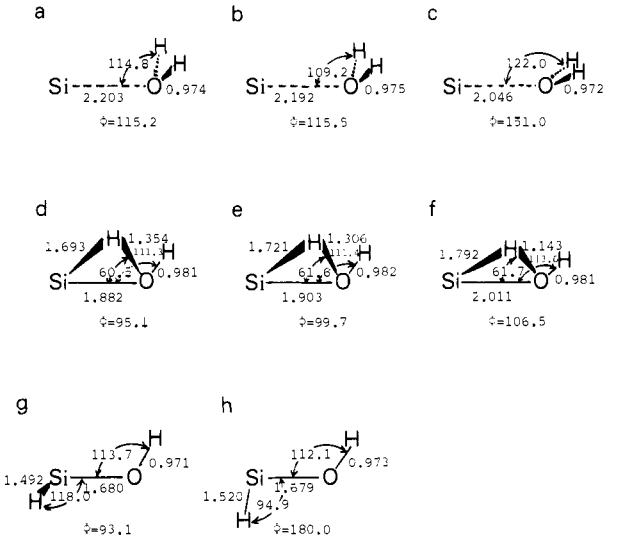

Figure 1. The MP2/6-31G* optimized geometries in Å and deg for (a) triplet silicon–water adduct (Cs), SiW($^3A''$); (b) open-shell singlet silicon–water adduct (Cs), SiW($^1A''$); (c) closed-shell singlet silicon–water adduct (Cs), SiW($^1A'$); (d) triplet TS of reaction 4, TS(triplet); (e) open-shell singlet TS of reaction 5, TS(open-singlet); (f) closed-shell singlet TS of reaction 6, TS(closed-singlet); (g) triplet *trans*-hydroxysilylene, HSiOH(triplet); (h) closed-shell singlet *trans*-hydroxysilylene (Cs), HSiOH($^1A'$). Φ is the dihedral angle H–Si–O–H.

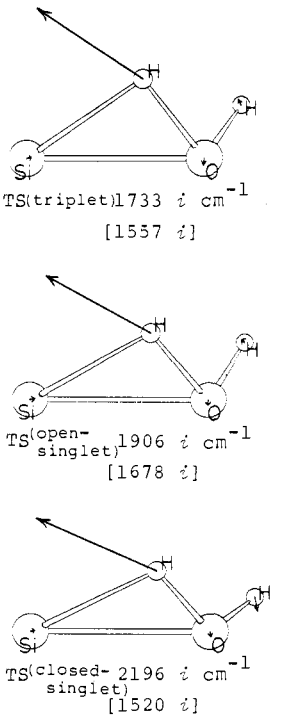

Figure 2. Imaginary vibrational mode and frequency of each TS by HF/6-31G*//HF/6-31G* [MP2/6-31G*//MP2/6-31G*].

(7) (a) Marcus, R. A.; Coltrin, M. E. *J. Chem. Phys.* **1977**, *67*, 2609. (b) Marcus, R. A. *J. Phys. Chem.* **1979**, *83*, 204.
(8) See, for example: (a) Fukui, K. *Acc. Chem. Res.* **1981**, *14*, 363. (b) Tachibana, A.; Fukui, K. *Theor. Chim. Acta (Berlin)* **1979**, *51*, 189.
(9) Binkley, J. S.; Frisch, M. J.; DeFrees, D. J.; Raghavachari, K.; Whiteside, R. A.; Schlegel, H. B.; Fluder, E. M.; Pople, J. A. GAUSSIAN 82, release A version, An Ab Initio Molecular Orbital Program, Carnegie-Mellon University, Pittsburgh, PA, September 1983.
(10) (a) Schlegel, H. B. *J. Comput. Chem.* **1982**, *3*, 214. (b) Schlegel, H. B. *J. Chem. Phys.* **1982**, *77*, 3676.
(11) Francl, M. M.; Pietro, W. J.; Hehre, W. J.; Binkley, J. S.; Gordon, M. S.; DeFrees, D. J.; Pople, J. A. *J. Chem. Phys.* **1982**, *77*, 3654.
(12) Dupuis, M.; King, H. F. *J. Chem. Phys.* **1978**, *68*, 3998.
(13) (a) Pople, J. A.; Binkley, J. S.; Seeger, R. *Intern. J. Quantum Chem.* **1975**, *9*, 229. (b) Pople, J. A.; Krishnan, R.; Schlegel, H. B.; Binkley, J. S. *Ibid.* **1979**, *S13*, 225.
(14) (a) Krishnan, R.; Pople, J. A. *Intern. J. Quantum Chem.* **1978**, *14*, 91. (b) Pople, J. A.; Krishnan, R.; Schlegel, H. B.; Binkley, J. S. *Ibid.* **1978**, *14*, 545. (c) Krishnan, R.; Frisch, M. J.; Pople, J. A. *J. Chem. Phys.* **1980**, *72*, 4244. (d) Frisch, M. J.; Krishnan, R.; Pople, J. A. *Chem. Phys. Lett.* **1980**, *75*, 66.

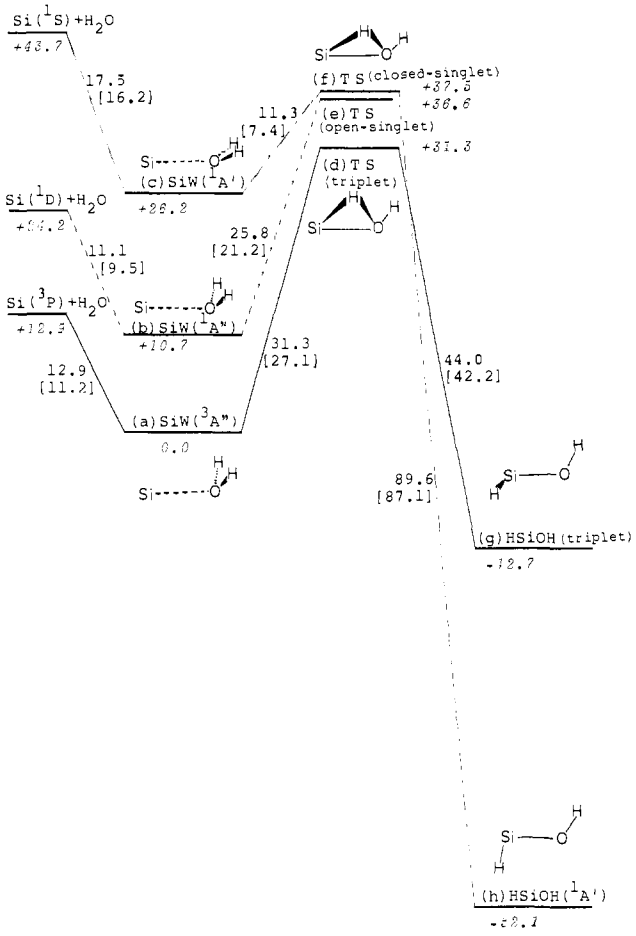

Figure 3. Schematic comparison of energy profiles in kcal/mol by MP4(SDTQ)/6-31G**//MP2/6-31G*. The italic values of each equilibrium point give the energies relative to the SiW(^{3}A"). Full line shows triplet UMP4//UMP2 energies. Dotted line shows open-shell singlet UMP4//UMP2 energies. Dashed line shows closed-shell singlet RMP4//RMP2 energies. The values along these lines stand for the energy barriers (E_a), while those in brackets are corrected E_a values for zero-point vibrational energies by MP2/6-31G*//MP2/6-31G*.

singlet) (part e) is an intermediate geometry between the TS-(triplet) (part d) and the TS(closed singlet) (part f).[15] On the other hand, the insertion product HSiOH(^{1}A') of the closed-singlet reaction is quite different from the triplet HSiOH.[5] HSiOH(^{1}A') is a planar trans isomer as shown in Figure 1h, and HSiOH(triplet) has out-of-plane H atom of Si–H as shown in Figure 1g. The latter geometry is close to the singlet TS between *cis*-HSiOH(^{1}A') and *trans*-HSiOH(^{1}A').[4] These features are similar to the results of HF/3-21G calculations for the carbon–water system analyzed by Ahmed et al.[16]

B. Relative Potential Energies and Reaction Barriers. The total energies and the ZPE corrections at the optimized geometries are listed in Table I. The MP4 potential energy profiles are schematically shown in Figure 3. The ground triplet state SiW(^{3}A") is 10.7 kcal/mol more stable than the open-shell singlet SiW(^{1}A"). The reaction starts at the triplet SiW(^{3}A"). When Figure 3 is searched from left to right, the triplet surface is lower till reaction goes over the TS(triplet). The triplet surface crosses both of the open- and closed-singlet surface near HSiOH. After going over the TS, the reaction path may be shifted on the singlet surface through the intersystem crossing. The subsequent reaction proceeds on the singlet surface. This theoretical picture agrees quite well with the mechanism suggested by the experiment[2] as described in section I.

On the singlet potential energy surface, the thermal decomposition of HSiOH(^{1}A') should be a two-step reaction: HSiOH(^{1}A') → $H_2Si{=}O$ → H_2 + SiO. The estimated energy barriers of these reactions are 63.2 and 85.8 kcal/mol, respectively.[4] Both reaction barriers are too high to allow the thermal process. Indeed, $H_2Si{=}O$(^{1}A') was not detected by IR spectra; irradiation was necessary for decomposition of HSiOH(^{1}A').[2] In the case of formaldehyde, the corresponding values are 28.3 and 79.6 kcal/mol, respectively.[17]

C. Reaction Path and Isotope Effect on the Proton Transfer. Reaction process 4 reveals interesting movement of the charge distribution along the reaction path. Table II shows the change of the atomic net charge along the IRC. The unit of the IRC is amu$^{1/2}$·bohr, and the TS is located at s = 0.0, where s is the distance measured along the IRC. The minus(plus) sign of s indicates the reactant(product) cell[8b] of the reaction. As shown in Table II, the migrating hydrogen is largely protonic in the early stage of the reaction process. Moreover, as shown in Figure 2, the displacement vector of the IRC at the TS demonstrates the major contribution from the migrating hydrogen's motion. Hence, the reaction process 4 is a proton transfer from water to silicon in the early stage. This migration process can be significantly affected if we replace the migrating hydrogen with deuterium. These characteristic features of the reaction clearly support the large kinetic isotope effect of the tunneling mechanism suggested by the experiment.[2] We study this isotope effect in detail, the same way as our previous work for the double-proton exchange in the formamidine–water system.[18]

Analysis of the IRC. The potential profile and the change of gradient norm and geometry along the IRC are shown in Figure 4 (part a–d). The gradient norm is defined as

$$N_g = \sqrt{\sum_{i=1}^{3N}(\partial W/\partial X^i)^2}$$

where N, W and X^i are the number of atoms, the potential energy, and the ith Cartesian coordinate, respectively. The change of gradient norm shows the force profile along the reaction process.

From Figure 4, it is seen that the deuteriation effect is large along the whole reaction bath. The reaction systems which have a migrating D atom have a much wider potential barrier than the H-migrating systems as shown in Figure 4a. The deviation of the potential curves for the H and D migration becomes larger as the reaction proceeds in the product region after TS, where the HSi bond forms. As shown in Figure 4b, the gradient norm has a higher peak before TS than after TS both for D and H migration. It is necessary for migration to occur more drastically before rather than after TS. Both peaks of gradient norm curves before and after TS are lower for D than for H. The process of H-migrating system has steeper potential barrier. Before TS, both peaks of gradient norm curves of D and H have the same position. After TS, however, the peak of one of D comes later than that of H. Consequently, the difference between the H-migrating system and the D-migrating system appears after TS rather than before TS. The migration of deuterium in the D-migrating system proceeds more slowly after TS. This is consistent with the potential profile as mentioned before.

The change of geometry along the IRC is shown in Figure 4 (parts c and d). Before TS, the OH distance remains almost constant, and the HOSi bending motion is the dominant process. After TS, the decrease of SiH length and HOSi angle is small, but the increase of OH length and HSiO angle is large. Hence, the clavage of the OH bond is dominant. The isotope effect emerges in this cleavage motion after TS more clearly than in the HOSi bending motion before TS. This corresponds to the

(15) The C_1 singlet excited state cannot be obtained at the UHF or UMP2 levels, in principle. In the present case, the structure (e) and (f) have a out-of-plane H atom in the plane almost perpendicular to the molecular plane, and these molecular structures would maintain the molecular symmetrylike plane, then the C_1 singlet excited state (f) can be obtained.

(16) Ahmed, S. N.; McKee, M. L.; Shevlin, P. B. *J. Am. Chem. Soc.* **1983**, *105*, 3942.

(17) Frisch, M. J.; Krishnan, R.; Pople, J. A. *J. Phys. Chem.* **1981**, *85*, 1467.

(18) (a) Marcus, R. A. *J. Chem. Phys.* **1964**, *41*, 603. (b) Yamabe, T.; Yamashita, K.; Kaminoyama, M.; Koizumi, M.; Tachibana, A.; Fukui, K. *J. Phys. Chem.* **1984**, *88*, 1459.

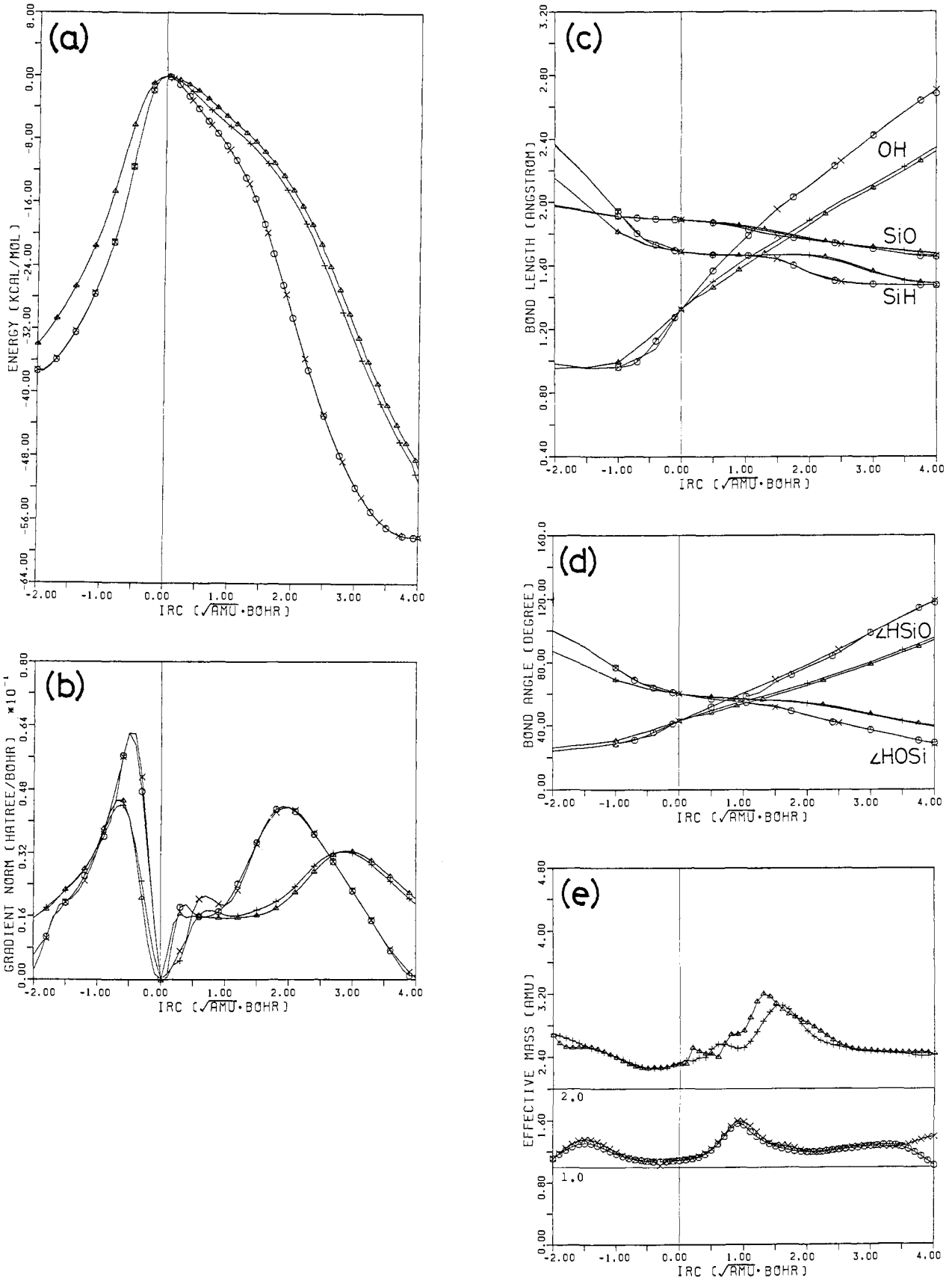

Figure 4. The IRC analysis for the reaction 4 of four isotopic species: (a) the potential profile, (b) gradient norm, (c) bond lengths, (d) bond angles, and (e) effective mass along the IRC. Meanings of the symbols are as follows: ○, Si:OH_2 → SiHOH → HSiOH (H-migrating system); ×, Si:OHD → SiHOD → HSiOD (H-migrating system); △, Si:ODH → SiDOH → DSiOH (D-migrating system); +, Si:OD_2 → SiDOD → DSiOD (D-migrating system).

Table II. Change of Net Charge on Each Atom Along IRC in Reaction 4 by UHF/6-31G*//UHF/6-31G*

	IRC (amu$^{1/2}$·bohr)											
atom	R[a]	−1.5	−1.0	−0.5	TS[a]	+0.5	+1.0	+1.5	+2.0	+3.0	+3.5	P[a]
Si	−0.099	−0.194	−0.199	−0.144	+0.129	+0.266	+0.319	+0.382	+0.435	+0.471	+0.465	+0.456
O	−0.863	−0.823	−0.810	−0.803	−0.777	−0.752	−0.801	−0.863	−0.872	−0.861	−0.846	−0.836
H[b]	+0.481	+0.511	+0.502	+0.443	+0.165	+0.010	+0.013	+0.019	−0.017	−0.073	−0.087	−0.092
H[c]	+0.481	+0.506	+0.507	+0.504	+0.483	+0.476	+0.468	+0.462	+0.454	+0.462	+0.468	+0.472

[a] The R, TS, and P mean reactant, transition state, and product, respectively. [b] Migrating hydrogen. [c] Hydrogen attached to oxygen.

change of the gradient norm in Figure 4b, where the delay of the peak in the D-migrating system emerges after TS rather than before TS. On the other hand, the heavy atom motions are dull. The degree of decrease in the SiO length is, however, largest at s = 1.0 and 1.5 in the H-migrating system and the D-migrating system, respectively.

The characteristics of the IRC will be further clarified by the analysis of effective mass and tunneling probability in the following sections.

Effective Mass in the Vicinity of TS. We calculated the effective mass $M^\ddagger$ along the IRC to consider the effect of mass of isotope.

The effective mass along the IRC is defined by[18]

$$M^\ddagger = G_{SS}/A_{SS}$$

where

$$G_{SS} = \sum_{i=1}^{3N} M_i \left(\frac{\partial X^i}{\partial s}\right)^2$$

and

$$A_{SS} = \sum_{i=1}^{3N} \left(\frac{\partial X^i}{\partial s}\right)^2$$

N, X^i, M_i, and s denote the number of atoms, ith Cartesian coordinate, its corresponding atomic mass, and the IRC, respectively. The effective mass is given in atomic mass units. It varies along the IRC because of the isotope effect and the heavy atom motion. We note also that a more accurate effective mass would involve contributions from reaction-path curvature,[19] which is not considered in this paper.

Figure 4e shows the change of the effective mass along the IRC. It is found that, in the H-migrating systems, the values of the effective mass are about 1.03∼1.6. The D-migrating system, however, has about twice as large a value, 2.3∼3.0. These results show that the principal contributions to the effective mass are the H atom and the D atom, respectively. The deviations from 1.0078 or 2.0141, which are the pure atomic masses of H or D, are caused by heavy-atom motion. The latter effect increases after TS, especially around s = 1.0 for the H-migrating system and s = 1.5 for the D-migrating system. The delay of the peak in the D-migrating system corresponds to the delay in the degree of decrease in the SiO length as mentioned in the discussion of geometrical change.

Since the effective mass depends sharply on the mass of the migrating atom and the reaction coordinate is mainly a migrating hydrogen atom motion, the tunneling effect of hydrogen should play an important role in this reaction process. A large isotope effect is then expected to be brought about. This will be examined in the next subsection.

Tunneling Probability. Finally, we estimated the tunneling probability semiclassically. The probability P for tunneling through a potential barrier is given as[7]

$$P = e^{-2\theta}$$

where θ is the action integral

$$\theta = \frac{1}{\hbar}\int_{s_1}^{s_2} ds[2\mu\{V(s) - E\}]^{1/2}$$

The limits s_1, s_2 are the classical turning points, which are determined numerically by solving $V(s) - E = 0$ for each total energy. Originally, the kinetic energy is assumed to be $V(s) + E_0(s) - E$, where $E_0(s)$ is the local vibrational zero-point energy for the bound vibrational modes orthogonal to the reaction path at s.[7a] The $E_0(s)$ may not be changed much on s; the calculation of $E_0(s)$ is beyond the scope of this paper, and we do not consider the effect of $E_0(s)$. The action integrals are calculated by using the Simpson formula. μ is the reduced mass of the reacting system which is euqal to unity along the IRC. The logarithm of the tunneling coefficient P is shown in Figure 5 as a function of the total energy difference from TS. There are also the critical difference between the H-migrating systems and the D-migrating ones. The latter have smaller tunneling effects than the former. The two H-migrating systems have almost the same profile. The two D-migrating systems have a slight deviation from each other. The difference between the two groups becomes larger as the total energy decreases below TS. It depends strongly on the effective mass of these systems or the width of the potential barrier. The larger the effective mass or the wider the potential barrier the system has, the smaller tunneling probability it has.

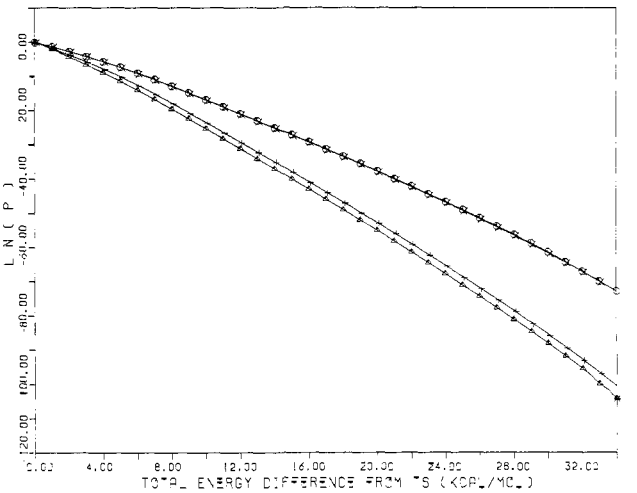

Figure 5. Logarithm of the total energy difference from TS. Tunneling coefficients for reaction 4 as a function of total energy difference from TS (○, ×, △, +) are the same as Figure 4.

IV. Conclusions

A large isotope effect is observed in the reaction path for the interaction of the silicon atom and the water molecule. Proton tunneling is the key to understanding the reaction mechanism. The intrinsic reaction coordinate approach is successfully used to elucidate the character of the reaction path. Water reacts with silicon in the triplet state (reaction 1), and proton tunneling occurs on the triplet potential energy surface (reaction 4). The migration of D from the silicon–water adduct is severely inhibited as is shown in the small tunneling probability. This corresponds to the experimental fact that DSiOH or DSiOD are not detected.[2] Intersystem crossing to the singlet surface may be effective to stabilize the migrated species HSiOH(triplet), which is expected to be examined in the future.

Acknowledgment. This work was supported by a Grant-in-Aid for Scientific Research from the Ministry of Education of Japan, for which we express our gratitude. The numerical calculations were carried out at the Data Processing Center of Kyoto University and the Computer Center of the Institute for Molecular Science (IMS).

(19) Truhlar, D. G.; Isaacson, A. D.; Skodje, R. T.; Garrett, B. C. *J. Phys. Chem.* **1982**, *86*, 2252.